Review #2 of Perez-Santos et al. – BG

Presented is a study of turbulent mixing and dissolved oxygen fluxes in the Patagonian fjords region. The topic is highly relevant, and the large number of microstructure profiles coupled with dissolved oxygen measurements covering the entire Patagonian fjords region across three distinct seasons is impressive. However, I don't quite follow the chosen formulation of the dissolved oxygen flux, which lacks adequate flux units, and I find the presentation of the turbulence results lacking a robust assessment. The discussion and conclusion are limited to the region analyzed, and there is no attempt to broaden the findings to other systems. There's evidence of haste in the writing, and while reading, I was constantly distracted by inconsistencies in the presentation and/or missing details. Altogether, I believe the paper's analysis is a bit too light given the data's high relevance.

Major comments

1. Flux calculations
   Despite the given reference, it is hard to follow why you aim to model vertical oxygen fluxes (J) using the 2nd Fick's law. The quantity you report, d(O2)/dt, has units of mass/volume/time, whereas flux is the mass passing through a surface per unit time (i.e., with units of mass/area/time) and for vertical flux, it is modeled by the 1st Fick's law: J = –Kz·d(O2)/dz, where Kz is the vertical diffusivity. From your VMP measurements, you obtain coupled microstructure and fast oxygen measurements, which yield Kz and d(O2)/dz at high vertical resolution. I simply don't understand the choice to compute the derivative of J (although without the key negative sign in the formulation) in the vertical domain to obtain d(O2)/dt. Also, I'm not sure how to interpret this quantity — it would make sense in the control volume of a reactor, though. If the authors want to keep the current analysis, they should provide justification and have the editor find it sound. But in any case, I request that the authors also report fluxes using Fick's 1st law, as it would greatly benefit the broader community – you have all the information needed.

   Your definition of transport direction in terms of d(O2)/dt is also misleading because diffusive fluxes will occur against the gradient (i.e., from high to low concentrations) independently of how the concentration varies as a function of time. Regardless, I believe upward should be strictly toward the surface, downward toward the bottom, and the terms positive and negative should be dropped throughout the manuscript.

Given the type of measurements performed, I would have expected to find further calculations using the oxygen fluxes, particularly time scales. Using averaged flux estimates as boundary conditions for some of the hypoxic/anoxic deep basins and a simplified 1D solution of the diffusion equation (using an averaged diffusivity from your microstructure turbulence analysis), you could calculate time scales for substantial changes in oxygen concentrations due to vertical transport. I believe the same could also be achieved with a clever scaling. Comparing those time scales with the lateral intrusion time scales of modified water from the Jacaf channel into the Puyuhuapi fjord would be particularly interesting. This approach would allow you to discuss the relevance of vertical versus lateral mixing across the different semi-enclosed systems.

We have edited the section 2.3 of the manuscript. The new section read as fallowed:

2.2 Data Analysis

2.2.1 Turbulence measurements

The dissipation rate of turbulent kinetic energy (ε) obtained by the VMP-250 was derived from the vertical shear sensor records, using the equation described by Thorpe (2007) and implemented in the ODAS Matlab library for all microprofiler instruments developed by Rockland Scientific International (Lueck, 2013). The equation is as follows:

$$\varepsilon=\frac{15}{2}\nu\overline{\left(\frac{\delta u}{\delta z}\right)^2}=\frac{15}{2}\nu\int_0^{\infty}\Psi\ (k)dk, \qquad (1)$$

where, ν is the kinematic viscosity, u is the horizontal velocity, z is the vertical coordinate, and Ψ is the velocity shear spectrum in wavenumber, k, space. $\left(\frac{\delta u}{\delta z}\right)^2$

2.2.2 Dissolved oxygen fluxes calculation

Oxygen concentrations in the water column are altered by air-sea fluxes, physical transport, and biogeochemical processes that can consume and produce oxygen in the water column. Not considering the fluxes through the air-sea interface, but within the water column itself, the oxygen budget can be expressed by the following oxygen balance equation (Peña et al., 2010):

$$\frac{\partial O_2}{\partial t}+u\frac{\partial O_2}{\partial x}+v\frac{\partial O_2}{\partial y}+w\frac{\partial O_2}{\partial z}-\frac{\partial}{\partial x}\left(K_H\frac{\partial O_2}{\partial x}\right)-\frac{\partial}{\partial y}\left(K_H\frac{\partial O_2}{\partial y}\right)-\frac{\partial}{\partial z}\left(K\frac{\partial O_2}{\partial z}\right)+S=0 \qquad (2)$$

In equation 2 the first term is the local rate of change of oxygen concentration with respect to time. The second and third terms are horizontal advection of oxygen concentration and the fourth term is vertical advection. The fifth and sixth terms are horizontal diffusion where K_H is the horizontal eddy diffusivity and the seventh term represents vertical mixing where K is the vertical eddy diffusivity (referred to here as 'diapycnal eddy diffusivity' or just 'eddy diffusivity'). The final term, S, represents sources or sinks of oxygen by biogeochemical processes (photosynthesis, respiration, etc.). In areas with reduced advection and horizontal diffusion like fjords and semi-enclosed seas with shallow sills, vertical mixing is the sole mechanism that can cause oxygenation below the pycnocline, which is reduced in areas of strong stratification (Eilola et al., 2009). Therefore, in fjords we can simplify the oxygen budget to the following, where we are also neglecting the source/sink term due to limited data availability:

$$\frac{\partial O_2}{\partial t} = \frac{\partial}{\partial z}\left(K\frac{\partial O_2}{\partial z}\right) \quad (3)$$

This equation states that local changes in oxygen concentrations with time are balanced by vertical diffusion of oxygen. Within the vertical diffusion term (right hand side of equation 3) is the diffusive flux, $J = -K\frac{\partial O_2}{\partial z}$, which describes the amount of oxygen that will flow through a unit area in a unit of time, or the flux of oxygen between layers. If the diffusive flux is positive, *J>0*, this indicates that oxygen is increasing toward the surface, whereas if *J<0* this indicates that oxygen is increasing with depth. We will quantify both the diffusive flux, *J*, and the vertical diffusion term. Quantification of the latter term will extrapolate the diffusive flux to inform the accumulation or depletion rate of oxygen at a specific depth over time.

According to the formulation of equation 3, $\partial O_2/\partial t$ (what we will refer to from here on as 'oxygen flux') represents the rate of change of oxygen concentration at a specific depth over time. When the oxygen flux is positive ($\partial O_2/\partial t > 0$) the concentration of oxygen at the considered depth is increasing with time due to the oxygen entering that specific depth layer faster than it is leaving($\frac{\delta}{\delta z}(k\frac{\delta O_2}{\delta z} > 0$). In other words, mixing (or diffusion) is actively recharging that layer with oxygen. Conversely, a negative oxygen flux ($\partial O_2/\partial t < 0$) indicates that oxygen concentration at the specific depth considered is decreasing with time due to oxygen at that specific depth layer leaving faster than it is being replenished, leading to oxygen depletion ($\frac{\delta}{\delta z}(k\frac{\delta O_2}{\delta z} < 0$). Comparable methodologies have been employed in the Baltic Sea by Holtermann et al. (2022) and more recently in the oxygen minimum zone by Pinto-Juica et al. (2026). Notably, in both of these studies, turbulence and oxygen measurements were obtained independently using two separate instruments (e.g., microprofilers and CTDOs), introducing potential sources of temporal and spatial error. In contrast, the data presented in this manuscript enable the detection of oxygen fluxes with a single instrument (see Figure 2c), thereby facilitating the quantification of gas fluxes with enhanced accuracy.

The eddy diffusivity K was obtained from direct measurement of ε (Equation 1) using the VMP-250-RD. The vertical gradient of DO($\frac{\delta O_2}{\delta z}$) was measured with a JAC-CT and DO RINKO sensor incorporated in the same VMP-250. To quantify the eddy diffusivity, we use the following formulation (utilized in Monismith et al., 2018; Ross et al., 2019; Smyth, 2020; Spicer and Huguenard, 2020; Bailey et al., 2025):

$$K = \Gamma\frac{\varepsilon}{N^2} \quad (4)$$

in which $\Gamma = \frac{R_f}{1-R_f}$ is a mixing coefficient that is a function of the flux Richardson Number, R_f. The flux Richardson number is held constant at 0.2 following Monismith et al., (2018) and therefore the mixing coefficient value was held constant at $\Gamma = 0.25$. We realize that inherently R_f varies with space and time depending on the relative amount of shear versus buoyancy in the water column, but without the relevant velocity data throughout the water column, we could not quantify squared vertical shear and thus could not quantify time and space variability of R_f. Monismith et al. (2018) has shown with numerous datasets that the constant value of $R_f = 0.2$ holds in much of the ocean interior, depending on the value of the Buoyancy Reynolds Number (or Activity Number, Gibson, 1980), which is calculated as,

$$Re_b=\frac{\epsilon}{\nu N^2} \quad (5)$$

where ν= 1.9 × 10^{-6} m^2 s is the molecular viscosity. In Knight Inlet in British Columbia Gargett et al., (1984) found that if Re_b>200 turbulence is unaffected by stratification (mixing occurs) if 15 < Re_b < 200 the effects of stratification become more important (starting to hinder mixing) and if $Re_b < 15$ stratification "kills turbulence". Monismith et al. (2018) found that if $Re_b <$ (100), then we can assume that the flux Richarson number, R_f, and thus Γ can be held constant. The mixing coefficient, Γ, is then used to quantify the eddy diffusivity. The buoyancy frequency (N^2) was calculated according to Stewart (2002):

$$N^2 = -\frac{g}{\rho}\frac{\partial\rho}{\partial z} \quad (6)$$

where g is the gravitational acceleration (m s^{-2}), ρ is the neutral density (kg m^{-3}), and ∂ρ/∂z is the vertical density gradient. The buoyancy frequency, also called Brunt-Vaisala frequency, was expressed in s^{-2}, and unstable values ($N^2 < 0$) were eliminated to reduce spikes in the K calculations. Densities were calculated using TEOS-10 formulas (IOC et al, 2010) with salinity anomalies derived from the atlas of Mcdougall et al. (2012). Results showed very low values of salinity anomalies in the range of 10^{-4} with seasonal average of 3.83×10^{-4} g kg^{-1} (March 2023), 3.73×10^{-4} g kg^{-1} (June 2023), and 3.90×10^{-4} g kg^{-1} (August 2023). Additionally, absolute salinity (S_A, units of g kg^{-1}) and conservative temperature (Θ in units of °C) were calculated to better represent the spatial variation of the different thermodynamic properties (IOC et al, 2010). The original N^2 values were retained without modification. However, the calculation of the vertical diffusivity (equation 4) and buoyancy Reynolds number (equation 6) were restricted to stably stratified conditions with $N^2 > 1\times10^{-5}$ s^{-2}. Values below this threshold were excluded because, under neutral, unstable, or very weakly stratified conditions, the inverse dependence on N^2 makes both quantities highly sensitive to small variations in stratification and may produce disproportionately large estimates. Similar screening criteria have been applied in previous turbulence studies, although with thresholds adapted to the characteristics and resolution of each dataset (e.g., Monismith et al., 2018; Goto et al., 2021; Piccoloraz et al., 2021). The threshold adopted here was selected from the observed N^2 distribution to distinguish weak near-neutral fluctuations from resolved stable stratification.

2. Lack of robust assessment of turbulence estimates and further analyses

Spectral fitting is difficult and prone to analytical errors. My impression is that no effort was made to convince the reader that the data were treated to the highest possible standards. I understand that, since the paper was submitted to Biogeoscience, details of the microstructure procedures may have been omitted because they are not the journal's primary focus. However, I'd like to see some evidence in the Appendix showing you really know what you're doing. Answering some specific questions detailed below may help.

- What binning was used for the turbulence microstructure analysis, e.g., 2-3 m, or was it a constant time window? Are the general characteristics of the turbulence profiles preserved if you increase or decrease the binning? Also, did you use any windowing? ATOMIX may suggest otherwise, but I would use an FFT window of 1/3 the bin length with a 50% overlap to obtain 3 spectra that are then averaged. The resulting averaged spectrum is then used to estimate epsilon using the Nasmyth procedure. This is done to ensure the reliability of the provided estimates.

We edited part of section 2.1 of the manuscript.

This instrument is equipped with high-response temperature (FP07) and water conductivity (SBE7) probes, as well as two vertical shear probes used to estimate the turbulent kinetic energy dissipation rate through fitting of the empirical Nasmyth spectra. The VMP measured the vertical shear of horizontal velocity in two orthogonal directions (∂u/∂z and ∂v/∂z) using two shear probes installed in the nose cone of the instrument (Fig. 2b). The instrument operated in a downward profiling mode, recording data at a sampling rate of 512 Hz as it descended at an optimal free-fall speed of approximately 0.7 $m\ s^{-1}$. As part of the data quality control procedures, a minimum profiling speed of 0.2 $m\ s^{-1}$ and minimum profile duration of 20 seconds were required for a cast to be considered valid. For the computation of the Nasmyth spectrum (Figure A1), the dissipation length was set to 8 seconds. The overlap of each dissipation estimate was set to 4 seconds. The time duration of the fft-segments ensemble-averaged for the wavenumber spectra was set to 2 seconds. The rate of dissipation above which the function will switch from the method of spectral-integration to the method of fitting to the inertial subrange, to estimate the rate of dissipation was set to 1.5×10^{-5} W kg^{-1}. The order of the polynomial used to compute the upper limit for integration was set to 3 over the spectra. The high-pass filter cutoff frequency for the shear probe data was 0.4 Hz, the low-pass filter cutoff was 30 Hz, and the anti-aliasing filter cutoff was 98 Hz. Corrections for vibrations were performed following the method described by Goodman et al. (2006). Data were excluded when the instrument's inclination angle exceeded 5% (Lueck et al., 2013), and post-processing followed the ATOMIX guidelines (Lueck et al., 2024). As part of quality control during VMP data analysis, probe estimates at each depth were compared. If one probe measurement exceeded the other by a factor of two, the larger estimate was removed from the records, following the approach of Stips (2005).

- Including some spectral fits in the supplementary material (for bins that pass and fail the spectral fit) would help the reader understand how finicky microstructure measurements are and therefore appreciate the effort put into assembling this dataset for the analysis of vertical transport of dissolved oxygen.

We included in the Index section the spectral analysis to stations added to the new Fig. 9.

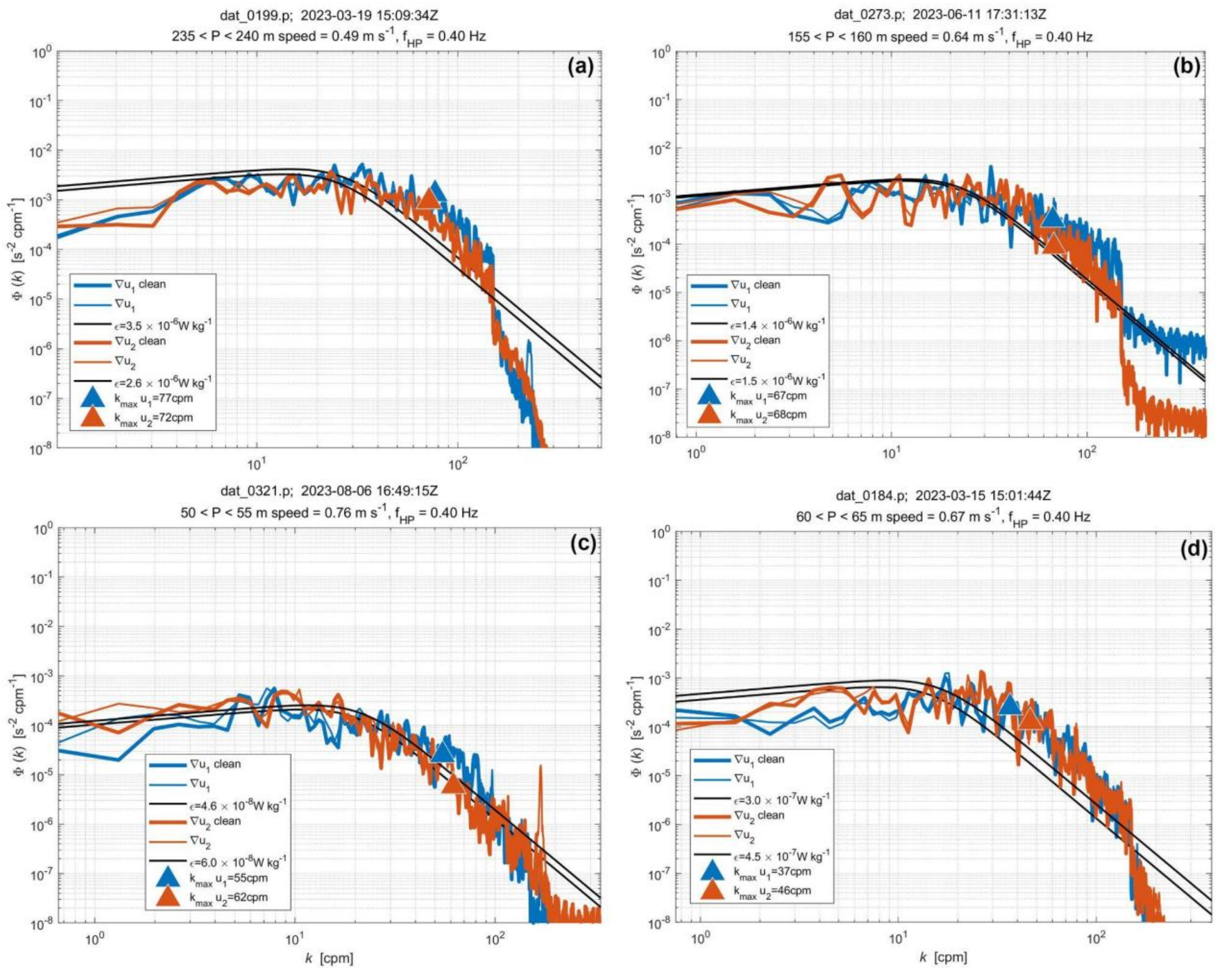

Figure A1. (a-d) Spectra of velocity shear (∂u/∂z) for shear probe 1 (blue line) and shear probe 2 (red line) in wavenumber space in the Chiloé Inner Sea at station E16 during (a) March 2023, (b) June 2023, and (c) August 2023, respectively, and (d) at station E30 in Puyuhuapi Fjord during March 2023. The black line denotes the dimensional Nasmyth spectrum, and the red and blue triangles denote the cut-off of maximum wavenumber (kmax) for each shear probe. The shear spectra were carried out in one of the intense turbulence layers for all profilers.

- It might be helpful to share with the reader how much data was discarded during QA/QC procedures. I did not see any NaN values in the reported epsilon profiles of your open-access data, which made me suspicious about QA/QC. Also, highlighting how closely the estimates from the quasi-independent shear probes matched would be a nice addition. In general, if the agreement between the two independent estimates is within a factor of 10, one reports the average value; otherwise, one discards the higher value.

As part of quality control during VMP data analysis, probe estimates at each depth were compared. If one probe measurement exceeded the other by a factor of two, the larger estimate was removed from the records, following the approach of Stips (2005). During this process, stations E10 (March 2023), E34 and E54 (June 2023), and E20, E50, E33, and E11 (August 2023) were repeated.

- I understand the paper is about diapycnal mixing, but from a superficial literature review, I gather that horizontal transport of different water masses sustains the hypoxic/anoxic layers in the Patagonian fjord system. It would be very nice if you could also quantify lateral dissolved oxygen fluxes due to isopycnal mixing (see the possible methodology in Fernandez Castro et al. 2025) and compare them with vertical transport through diapycnal mixing. I understand if this may feel like part of a completely different paper, but I am commenting because it could offer new insight. I believe it at least warrants discussion.

  Fernández Castro, B., Fernández Román, D., Ferron, B., Fontela, M., Lherminier, P., Naveira Garabato, A., et al. (2024). Isopycnal eddy stirring dominates thermohaline mixing in the upper subpolar North Atlantic. Journal of Geophysical Research: Oceans, 129, e2023JC020817. https://doi.org/10.1029/2023JC020817

  We thank the reviewer for this new idea that will be part of our next research. See section of Limitations in the Discussion.

3. Numerical model

   The model is disconnected from the paper. From my reading, it is mostly used to show that the Chiloe inner sea is energetic, and that explains the elevated turbulence estimates in that region compared to the rest of the dataset presented. However, since the model has been validated and published elsewhere, all this could be a sentence in the discussion or, at best, the material moved to the supplementary. Moreover, in Fig. 10c, you are comparing field estimates and model results for quantities with different units, and, as expected, since you are mingling scales, the quantities do not show agreement. Altogether, in my opinion, you would need to further develop your ideas and analyses to justify including the model results. One idea would be to use it to calculate residence times for layers with distinct oxygen levels across the different semi-enclosed basins to assess the relative importance of lateral transport versus vertical mixing. I have the impression that vertical transport may dominate in single-mouth fjords with a sill, but in the Jacaf-Puyuhuapi system, lateral oxygen transport from the adjacent deep, wide channel may dominate instead.

We agree with the reviewer that, in the previous version of the manuscript, the contribution of the numerical model was not sufficiently connected to the turbulence observations. We therefore further developed the model analysis and revised Section 3.4 and Figure 10 to better evaluate the relationship between tidal forcing and the observed turbulent dissipation. We clarify that the comparison between modeled KE_{M2} and observed ε is not intended as a direct model–observation validation or agreement between equivalent quantities, since they represent different physical variables and different spatial and vertical scales. Instead, the purpose of the comparison is to evaluate whether locations characterized by stronger modeled M2 tidal forcing are also associated with enhanced observed turbulent dissipation. In addition to the relationship using all available stations (Fig. 10c), we now include a new analysis focused on the most energetic tidal regions (Fig. 10d). High-tidal-energy stations were objectively defined as those within the upper quartile (Q75) of the March KE_{M2} distribution at the field station locations. The same station identities were then retained for the June and August campaigns. When all stations are considered, the log–log relationship between KE_{M2} and ε has $R^2 \approx 0.32$ and a slope of approximately 0.36. For the high-KE_{M2} subset, the relationship becomes more defined, with R^2 increasing to approximately 0.42 and the fitted slope increasing to approximately 1.00. Although considerable dispersion remains, this result indicates that enhanced M_2 tidal energy is more consistently associated with elevated turbulent dissipation in the most energetic passages and channels.

We also appreciate the reviewer's suggestion to estimate residence times for layers with different oxygen concentrations and to compare lateral transport with vertical mixing, particularly in the Jacaf–Puyuhuapi system. We agree that this would be a valuable analysis. However, the present model analysis is hydrodynamic and does not include an explicit dissolved-oxygen tracer; therefore, a robust basin- and layer-specific residence-time analysis would require an additional tracer or property-budget framework that is beyond the scope of the present study. We have therefore limited the interpretation of the model results to identifying the physical forcing associated with the observed turbulence, without implying that the model quantifies the complete oxygen budget or establishes the relative dominance of lateral versus vertical oxygen transport.

The corresponding text in Section 3.4 was revised as follows:

To quantify the relationship between tidal energy and turbulent dissipation, the median dissipation rate (ε) was computed for each station from the vertical profiles obtained during each of the 2023 field campaigns. These observational estimates were compared with the modeled tidal kinetic energy (KE_{M2}), interpolated from the model grid at each station location (Fig. 12b). The relationship was evaluated in log–log space to better resolve the wide range of variability (Fig. 12c). Because KE_{M2} and ε represent different physical quantities and spatial and vertical scales, this comparison is not intended as a direct model–observation validation, but rather to evaluate whether stronger modeled M_2 tidal forcing is associated with enhanced observed turbulent dissipation. Considering all available observations, the results show a positive association between KE_{M2} and ε, although with considerable dispersion spanning one to two orders of magnitude for a given tidal energy level. The least-squares fit in log–log space yields a slope of approximately 0.36 and $R^2 \approx 0.32$ (Fig. 12c).

To examine the relationship specifically within the most energetic tidal regime, stations within the upper quartile (Q75) of the summer KE_{M2} distribution at the field station locations were selected (white circles in Fig. 12b), and the same were retained for the fall and winter campaigns. For this high-KE_{M2} subset, the relationship becomes more defined, with R^2 increasing to approximately 0.42 and the fitted log–log slope increasing to approximately 1.00 (Fig. 12d). Although considerable dispersion remains, this strengthening of the relationship indicates that elevated M^2 tidal energy is more consistently associated with enhanced turbulent dissipation in the most energetic passages and channels. Overall, these results are consistent with the spatial patterns described above, suggesting that while tidal forcing provides an important energy source for turbulence, the magnitude of ε remains strongly modulated by local conditions such as stratification, bathymetry, and flow variability.

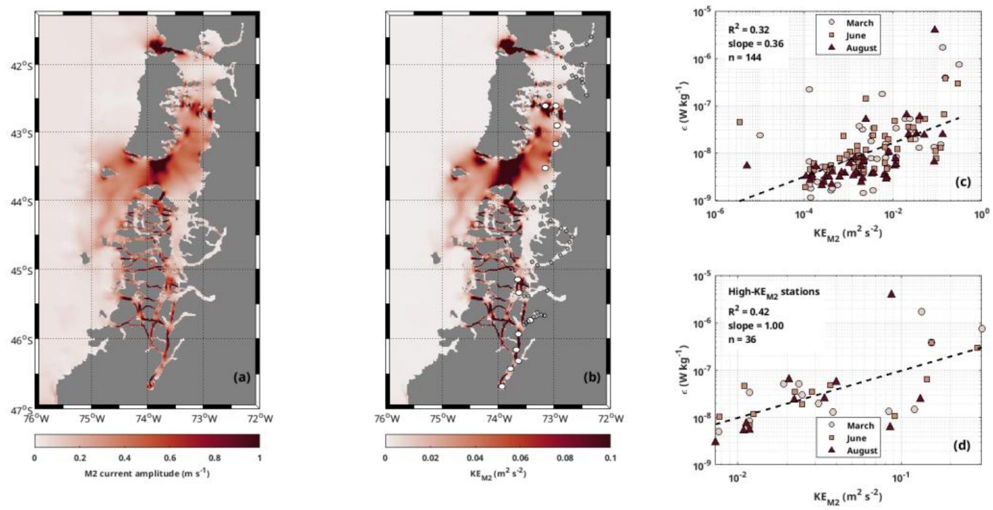

Figure 10. (a) Amplitude of the M_2 tidal current (m s⁻¹) derived from harmonic analysis of depth-averaged model velocities for March 2023. (b) Kinetic energy associated with the M_2 tidal current (KE_{M2}, m² s⁻²), computed from the amplitudes of the zonal and meridional components. (c) Relationship between modeled KE_{M2} and observed turbulent dissipation rates (ε, W kg⁻¹) at station locations for March (blue), June (red), and August (black) 2023. Dissipation values correspond to the median of vertical profiles at each station, and KE_{M2} was interpolated from the model grid. Both axes in (c) are shown in $\log_{10}$ scale. The dashed line indicates a least-squares fit in log–log space.Figure 10. (a) Amplitude of the M_2 tidal current (m s⁻¹) derived from harmonic analysis of depth-averaged model velocities for March 2023. (b) Kinetic energy associated with the M_2 tidal current (KE_{M2}, m² s⁻²), computed from the amplitudes of the zonal and meridional components. White circles indicate stations within the upper quartile (Q75) of the March KE_{M2} distribution at the field station locations used for the high-tidal-energy analysis. (c) Relationship between modeled KE_{M2} and observed turbulent dissipation rates (ε, W kg⁻¹) at all available station locations for March (circles), June (squares), and August (triangles) 2023. (d) Same relationship considering only the high-KE_{M2} stations identified in (b), with the same station identities retained across the three campaigns. Dissipation values correspond to the median of the vertical profile at each station, whereas KE_{M2} was interpolated from the model grid at the corresponding station location. Both axes in (c) and (d) are logarithmic. Dashed lines indicate least-squares fits in log–log space.

Minor comments

1. Broader context. While the introduction clearly and nicely states the relevance of mapping oxygen concentrations and understanding oxygen transport in the Patagonian fjords, the opening feels quite region-specific. I think the broader community would appreciate a brief review and contextualization of why the presented measurements and analyses are relevant to similar fjord systems (e.g., British Columbia, Scandinavia, and New Zealand). Moreover, I understand that Elin Darelius has been studying hypoxia in Norwegian fjords in recent years. I do not know whether that work has been published, but it would be interesting to compare.

We edited paragraph in the introduction section:

Fjord ecosystems exhibit heightened sensitivity to hypoxic conditions, typically defined as dissolved oxygen (DO) concentrations below 2 ml L⁻¹, equivalent to 30% oxygen saturation or 89 µmol L⁻¹. This susceptibility is particularly evident in settings with irregular topography, which can impede or inhibit deep-water ventilation, as observed by Jackson et al. (2021) in the British Columbia fjord system. In addition, extensive longitudinal studies by Aksnes et al. (2023) and Solas et al. (2025) focusing on the Masfjorden within the Norwegian fjord system have *provided critical insights into the processes of hypoxia, deoxygenation, and reoxygenation, elucidating the dynamics of DO under both natural and anthropogenic influences. More recently, Hare et al. (2026) identified and characterized the formation of a low-oxygen layer in a remote fjord within the British Columbia system, once again underscoring the centrality of fjord oxygen dynamics in current research across both northern and southern fjord belts. This persistent research interest is driven by mounting scientific concern regarding global ocean deoxygenation (Ferrer et al., 2025).*

2. For the transects performed within fjords, was any care taken to conduct entire transects during either ebb or flood tides? Measurements during different phases of the tidal cycle may encounter different currents that affect shearing layers and ultimately turbulence levels.

We agree with the comment and added the information on tidal moments in Table 1 of the manuscript:

Table 1. Oceanographic campaigns carried out in northern Patagonian (PN) fjords and channels.

Expeditions (Austral seasons)	**Date**	**Temperature, salinity, and DO_2 stations**	**Turbulence stations**	***Tidal coefficient/Date**	**Tidal moment**
PN-Summer	March 04-19, 2023	52	47	90 (higher)/ March 19, 2023	Neap tides
PN-Fall	May 30-June 14, 2023	56	55	61 (medium)/ June 11, 2023	Neap tides
PN-Winter	August 6-20, 2023	56	56	77 (high)/ August 6, 2023	Neap tides

*Tidal coefficient obtained during Chiloe Inner Sea turbulence measurements (E8 and E10).

3. Fig. 1. I'm colorblind and can't discern the information displayed there clearly. Aside from the color choice, it looks cluttered and seems to include information that may not be necessary (e.g., lakes and snow). The text and symbols are hard to read in both panels. I'd recommend changing the color palette, reducing the text and information to what is absolutely relevant, and using buffered text to improve readability. Also, you can check whether your figures are suitable for individuals with different types of colorblindness at: https://www.color-blindness.com/coblis-color-blindness-simulator/

We edited Figure 1 according to the comments.

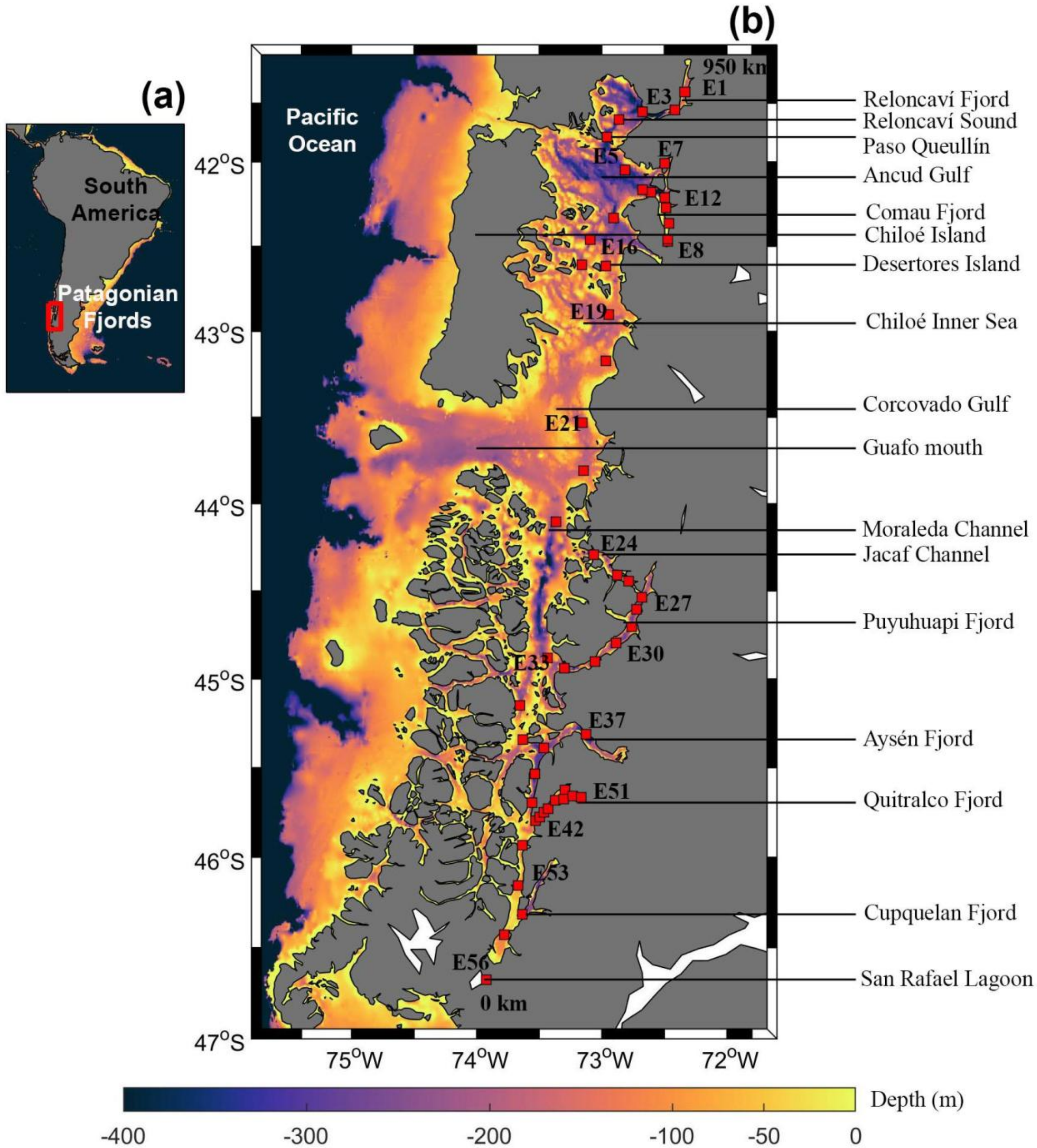

Figure. 1. (a) Map showing the fjords location in relation to South America and (b) the sampling stations carried out seasonality during 2023 in northern Patagonian fjords (all measurements described in Table 1). The rivers and lakes (blue), and snow cover (white) were added to the maps. The transect used to represent the results shown in Figures 3-6 is denoted with a continuous red line.

4. Table 1. Unclear. Alignment fails to provide information. Is it possible that the last row in the Measurements column, labeled 'Turbulence', is a typo? An in-text description is missing. Finally, were full transects performed at each campaign?

We edited the Table to clarify information:

Table 1. Oceanographic campaigns carried out in northern Patagonian (PN) fjords and channels.

Expeditions (Austral	**Date**	**Temperature, salinity, and**	**Turbulence stations**	***Tidal coefficient/Date**	**Tidal moment**

seasons)		**DO_2 stations**			
PN-Summer	March 04-19, 2023	52	47	90 (higher)/ March 19, 2023	Neap tides
PN-Fall	May 30-June 14, 2023	56	55	61 (medium)/ June 11, 2023	Neap tides
PN-Winter	August 6-20, 2023	56	56	77 (high)/ August 6, 2023	Neap tides

*Tidal coefficient obtained during Chiloe Inner Sea turbulence measurements (E8 and E10).

5. Lines 106-107: "…as well as two vertical shear probes (which measure mechanical turbulence in the water)". This is inaccurate; shear probes do not directly measure turbulence. They are used to estimate the turbulent kinetic energy dissipation rate through fitting of the empirical Nasmyth spectra. Please correct.

We edited the sentence.

6. Lines 106 and 121. What do you mean by high-response? FP07 is a fast thermistor with a short response time (Fast Probe 07 [ms] with a nominally 10 ms response time). For the DO probe, is there a way to convert that % definition into an equivalent response time? I don't understand what is meant there.

We included the answer of the technical team of Rockland Scientific:

"High-response" is not really a quantitative specification, so I would suggest replacing it with "fast-response" and giving the manufacturer's stated response time for the RINKO DO sensor.

JFE specifies a 90% response time of <1 s (in air at 25 degC). In other words, the 90% is the criterion used to define the response time: following a step change, the sensor reaches 90% of the final signal in less than 1 s. So there is not really a conversion from "90%" to a response time as the corresponding response time is already <1 s.

For reference on these response time values you can review the following links/sources on our website here:

- Rinko DO: https://rocklandscientific.com/products/jfe-advantech-co-ocean-river-instruments/
- FP07 Sensor: https://rocklandscientific.com/wp-content/uploads/2021/12/TN_005.pdf

I think the safest revision would simply be to state the actual manufacturer specifications rather than calling either sensor "high-response". For the FP07, Rockland gives a response of about 7 ms in water at a flow speed of 1 m/s (with response depending on flow speed); for the RINKO, t90 <1 s in air at 25 degC.

7. Section 2.2. This is an incomplete and misleading explanation of how TKE dissipation rates are obtained from microstructure shear measurements. Some important details are provided around lines 112-118. Merging all the turbulence methods into one section would be appreciated.

We edited section 2.2 of the manuscript.

8. Lines 148-152. It is stated here that eq. 3 is "the most frequently used formulation for Kshear" and Osborn (1980) is cited. This is incorrect. The most used formulation is by far that of Osborn (1980) using a constant diapycnal flux coefficient, Γ:

$$Kz = \Gamma\, \varepsilon / N^2$$

with Γ=0.2. Check the references below for further explanation of why this holds.

Monismith et al. (2018): https://doi.org/10.1029/2018GL077229

Smyth (2020): https://doi.org/10.1175/JPO-D-20-0083.1

We edited section 2.2 of the manuscript.

9. Fig 2: Make sure you mention that these images belong to Rockland (RSI) if that's the case.

We edited the caption of Fig 2. "***Figure 2. (a) Vertical microprofiler model VMP250-RDL with (b) two shear probes and one micro-temperature and micro-conductivity probe incorporated. (c) A fast-response DO sensor was integrated to quantify DO fluxes with the same instrument. The images were obtained from the Rockland Scientific user manual***".

10. All transect figures would benefit from the inclusion of bathymetry. For example, in Fig. 3, I infer that the stations are the same (not mentioned in the methods), but the profiles' depths differ.

We added the bathymetry contour to all figures in the manuscript, e.g.:

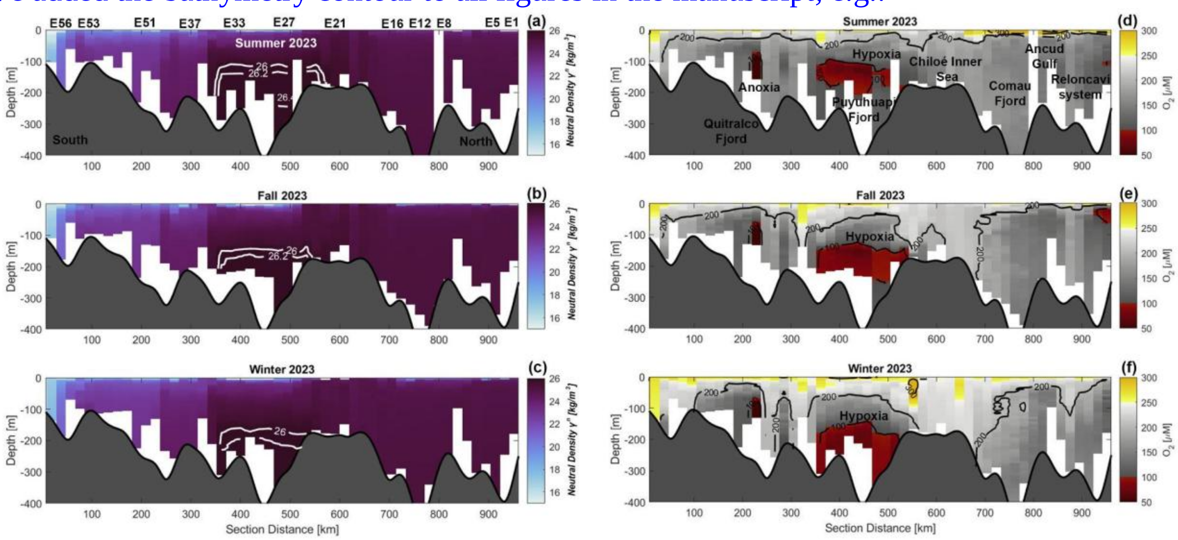

Figure 3. Seasonal vertical distribution of the (a-c) water density and (d-f) dissolved oxygen obtained from the San Rafael Lagoon (0 km, E56) to the Reloncaví Fjord (970 km, E1).

11. How do you calculate density? [If you use TEOS-10, has it been validated for Patagonian fjord waters?] Also, in the results section, you present density anomaly, but in Fig. 3,

density is presented as neutral density, which is a completely different quantity. I guess this is just a labeling mistake.

Densities were calculated using TEOS-10 formulas (IOC et al, 2010) with Salinity Anomalies derived from the atlas of Mcdougall et al. (2012). Results showed very low values of salinity anomalies in the range of 10^{-4} with seasonal average of $3.83 \cdot 10^{-4}$ g/kg (March 2023), $3.73 \cdot 10^{-4}$ g/kg (June 2023), and $3.90 \cdot 10^{-4}$ g/kg (August 2023).

- IOC, SCOR and IAPSO, 2010: The international thermodynamic equation of seawater - 2010: Calculation and use of thermodynamic properties. Intergovernmental Oceanographic Commission, Manuals and Guides No. 56, UNESCO (English), 196 pp. Available from http://www.TEOS-10.org See section 2.5 and appendices A.4 and A.5 of this TEOS-10 Manual.

- McDougall, T.J., D.R. Jackett, F.J. Millero, R. Pawlowicz and P.M. Barker, 2012: A global algorithm for estimating Absolute Salinity. Ocean Science, 8, 1117-1128.

We edited the error and changed "density anomaly" by "neutral density".

12. Buoyancy frequency and Brunt-Väisälä frequency are used interchangeably, e.g., in eq. 3 and Fig. 4, but are not defined as equivalent. I'd recommend using buoyancy frequency throughout the manuscript. It would also be appreciated if you included a definition of N^2 and the method used to calculate it. Note that, in several profiles I checked in your open data, N^2 appears to be a linear function, and for the reported range of values, the units must be in cph rather than $1/s^2$.

We edited the figure and added new information about the N_2 calculation in section 2.2. Additionally, we created a new dataset and uploaded it again.
https://doi.org/10.5281/zenodo.22133711

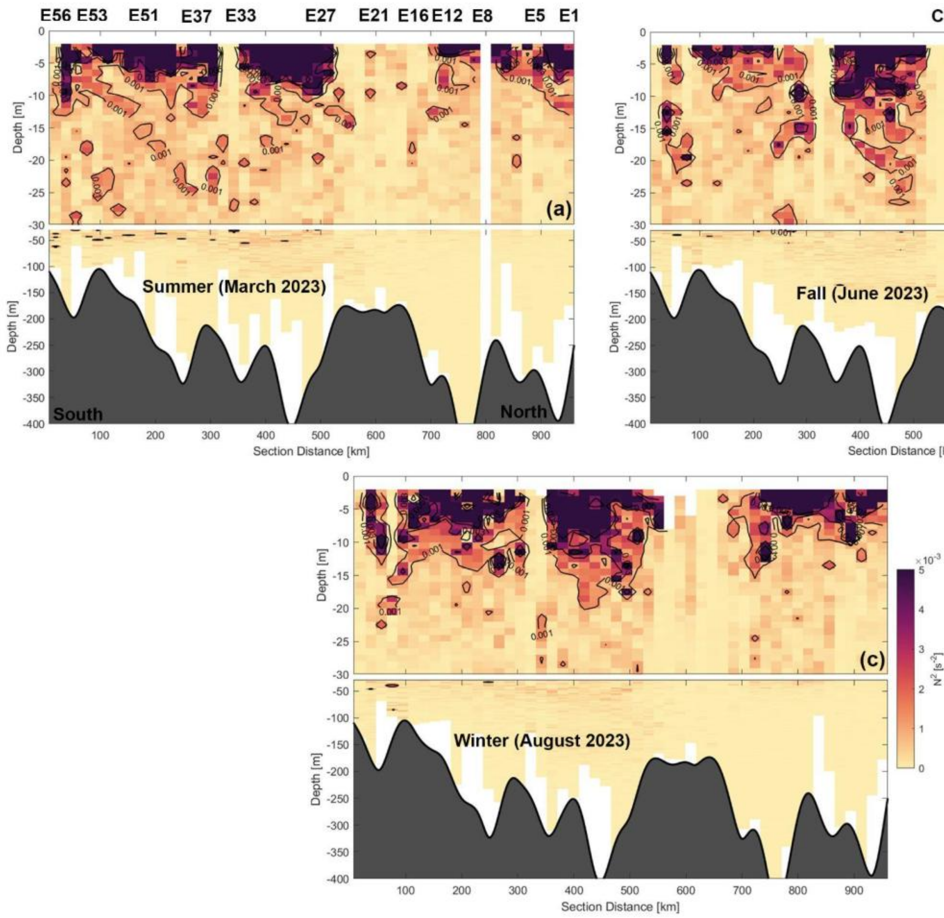

Figure 4. Seasonal records of the Brunt-Väisälä frequency along a vertical section in the northern Patagonian fjords (a) summer, (b) fall, and (c) winter during 2023.

> I also noted in your open data that some of the Kz profiles show spikes. I suspect some of those spikes are generated by locally unstable N^2 values that are being masked as very small values close to 0. A clever way to handle data when calculating K from dissipation and buoyancy frequency is to use an N^2 computed from a monotonically reordered (i.e., stable) density profile.

We recalculated K using only positive N^2 values. This new approach, as recommended by the reviewer, reduced the error.

13. Figs. 4 and 5. I don't see a compelling reason to use a diverging colormap in these figures. There's no clear pivot, such as a sign change or a marked regime shift. I'd suggest using a perceptually uniform, sequential colormap for these plots (e.g., cmocean matter).

We edited the figures.

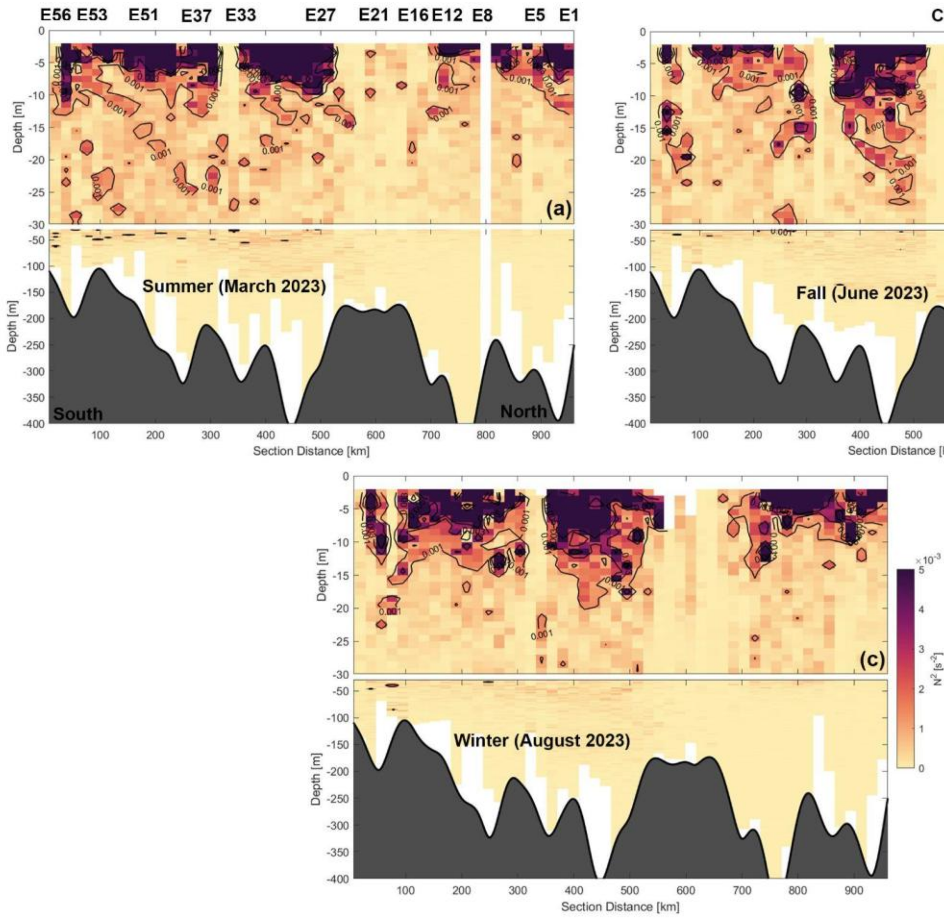

Figure 4. Seasonal records of the Brunt-Väisälä frequency along a vertical section in the northern Patagonian fjords (a) summer, (b) fall, and (c) winter during 2023.

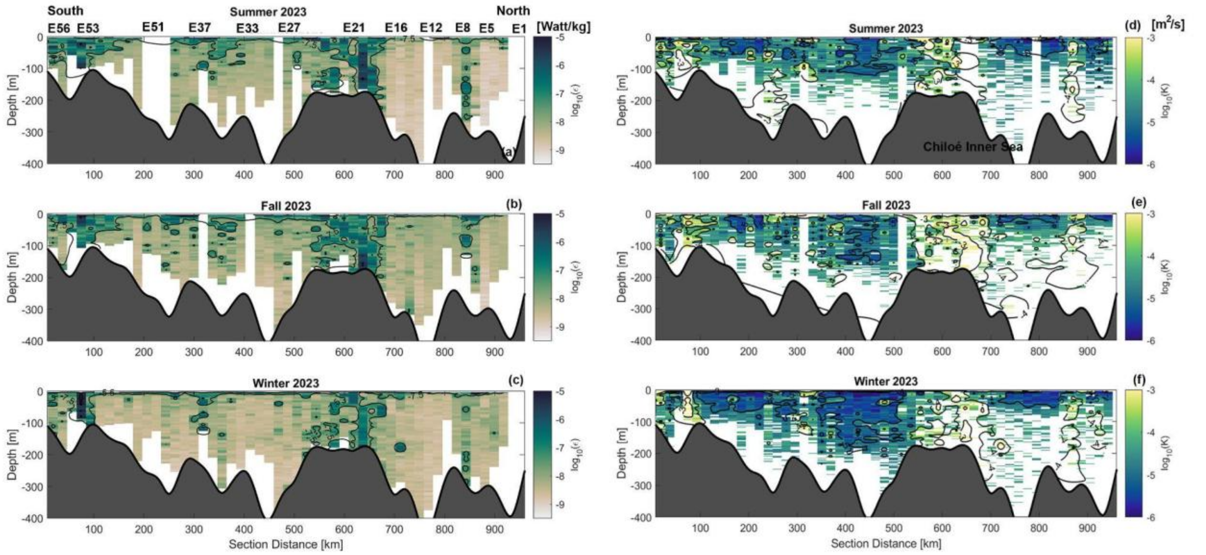

Figure 5. Seasonal vertical distribution of the (a-c) dissipation rate of turbulent kinetic energy and (d-f) diapycnal eddy diffusivity obtained from the San Rafael Lagoon (0 km, E56) to the Reloncaví Fjord (970 km, E1).

14. Figure 7. I really struggle to interpret this figure. For example, in the large bar near 200 m depth in panel (a), does this mean there are 0 values at 1.6 uM/s and 2 values at 1.9 uM/s? There must be a better way to show the seasonal differences noted in the in-text description.

We added a new figure.

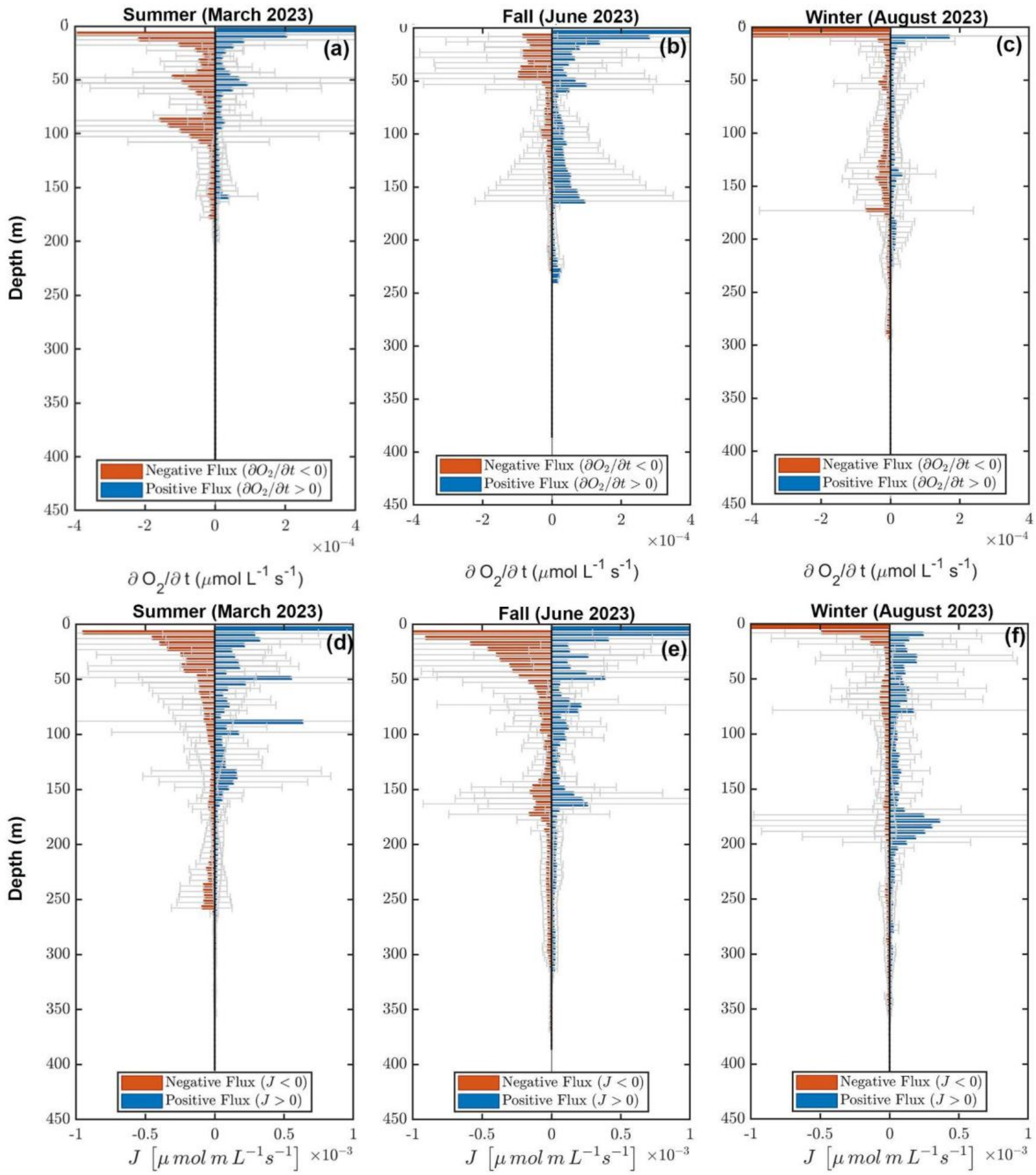

Figure 8. Average profile with standard deviation of negative and positive DO fluxes in the northern Patagonian fjords.(a-c) Shows results using the DO fluxes (∂O_2/∂t), and (d-f) DO diffusive flux (J).

15. Figure 8. After struggling to follow the lower panel of Fig. 8 and reviewing your open data, I realized that Figs. 8q, r and s are identical to Figs. 8l, m and n. That should be corrected.

Also, using the provided open data, e.g., the profile from Fig. 8p, I could not reproduce the reported Kz and d(O2)/dt profiles because the N^2 data are spurious (see minor comment 12 on N^2). Finally, what are those intermittent black lines in all the Kz profiles? Whatever the reason, this can definitely be handled better for presentation.

We added a new Figure including all comments and corrections.

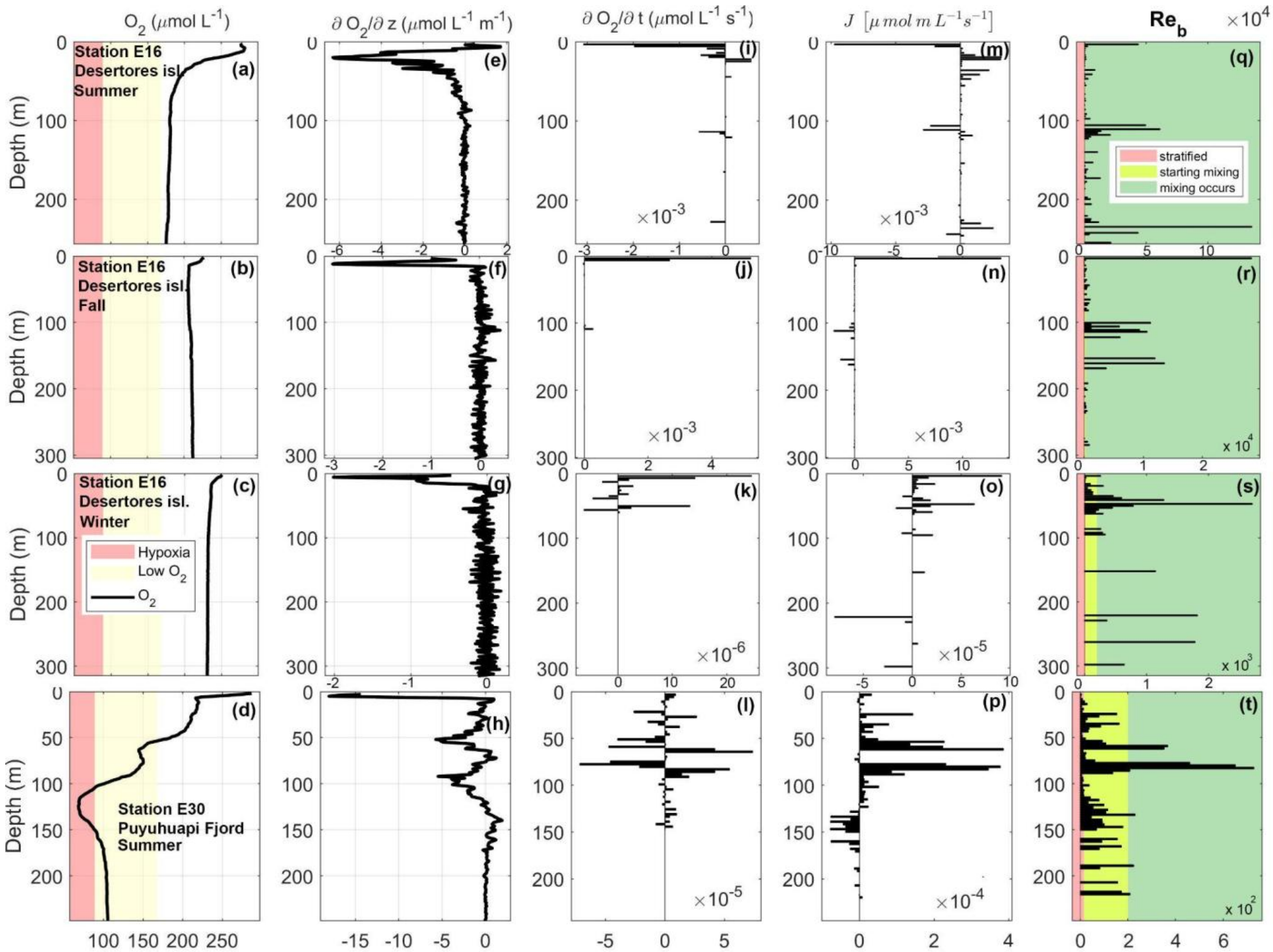

Figure 9. Examples of profiles of oxygen fluxes obtained at the intense turbulence mixing region in the Chiloé Inner Sea (E16) and in the hypoxic and ventilated region inside the Puyuhuapi Fjord (E30). (a-d) DO profiles, (e-h) DO vertical gradients, (i-l) DO flux, (m-p) DO diffusive flux, and (q-t) Reynolds number. We have kept the x-axes of each variable to observe the magnitude of each process.

16. T-S diagrams color coded for O2 concentrations and J = – Kz·d(O2)/dz for single-mouth fjords (grouped) and the Jacaf-Puyuhuapi system to compare the different water masses that may intrude into the basins vs diapycnal mixing would be interesting additions.

We added a new figure to describe and discuss the relationship between the T-S diagram and all calculated variables in the manuscript.

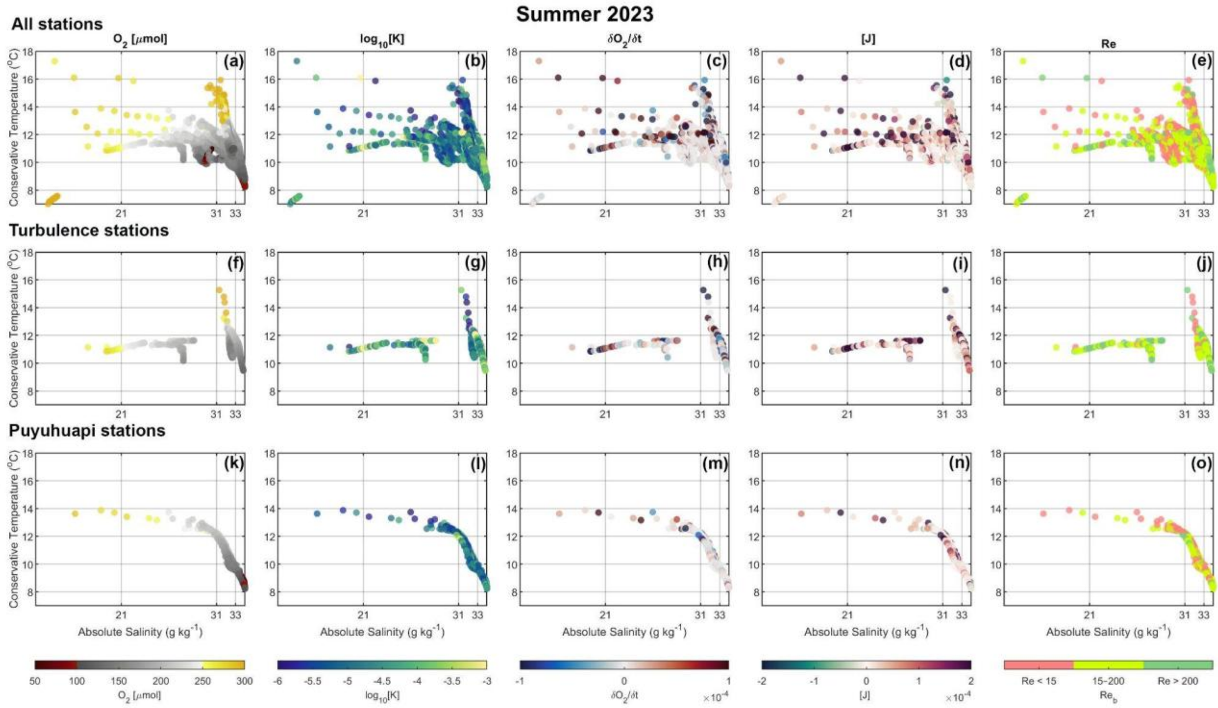

Figure 10. T-S diagrams vs diapycnal eddy diffusivity (K), vertical oxygen fluxes ($\partial O_2/\partial t$), diffusive flux of oxygen (J), and Reynolds number (Re_b) during March 2023. (a-e) Represented the data of all sampling stations; (f-j) stations where an intense dissipation rate of turbulent kinetic energy (ε) was detected, and (k-o) stations carried out in the Puyuhuapi Fjord.

17. Lines 458-466. I can't quite follow the proposed idea that double diffusion convection may play a role in diapycnal mixing processes of oxygen throughout the water column. You are working in a high-turbulence region and the resulting mixing would smooth out any signature of DDC at short timescales. The state of the art is quite categorical in that double diffusion may take place when background shear is negligible (Gregg et al. 2018), so the difference between the diffusivities of temperature and salinity remains 2 orders of magnitude. (i.e., at the molecular level). DDC would be expected in deep basins with low turbulence levels, but not in the upper regions as suggested in Fig A1,b and c. Layering in natural environments is ubiquitous. (e.g., Middleton et al. 2025). Turner angle alone is misleading because it only provides an after-the-fact indication that offers no information about the formation mechanism. Unless you can provide a theoretical framework that can help reconcile what you are stating about DDC, I think this bit does not belong here. You may, however, be in the presence of differential diffusion.

We agree with the comment and deleted all the information about the DDC in this manuscript.

M.C. Gregg, E.A. D'Asaro, J.J. Riley, E. Kunze. 2018. Mixing Efficiency in the Ocean. Annual Review of Marine Science 10:443-473. https://doi.org/10.1146/annurev-marine-121916-063643

Middleton L, Brown JM, Taylor JR. 2025. Reconciling layering mechanisms in double-diffusive and single-diffusive fluids. Journal of Fluid Mechanics 1019:R1. https://doi.org/10.1017/jfm.2025.10539